Function, Targets, and Evolution of *Caenorhabditis elegans* piRNAs

Marloes P. Bagijn,[1*] Leonard D. Goldstein,[1*†] Alexandra Sapetschnig,[1*] Eva-Maria Weick,[1] Samir Bouasker,[2] Nicolas J. Lehrbach,[1] Martin J. Simard,[2] Eric A. Miska[1‡]

[1]Gurdon Institute and Department of Biochemistry, University of Cambridge, The Henry Wellcome Building of Cancer and Developmental Biology, Tennis Court Road, Cambridge CB2 1QN, UK.

[2]Laval University Cancer Research Centre, Hôtel-Dieu de Québec (CHUQ), Quebec City, Québec G1R 2J6, Canada.

*These authors contributed equally to this work.

†Present address: Department of Bioinformatics and Computational Biology, Genentech Inc., 1 DNA Way, South San Francisco, CA 94080, USA.

‡To whom correspondence should be addressed. E-mail: e.miska@gurdon.cam.ac.uk

Piwi-interacting RNAs (piRNAs) are small RNAs required to maintain germline integrity and fertility but their mechanism of action is poorly understood. Here we demonstrate that *C. elegans* piRNAs silence transcripts *in trans* through imperfectly complementary sites. Target silencing is independent of Piwi endonuclease activity or "slicing." Instead, piRNAs initiate a localized secondary endogenous small interfering RNA (endo-siRNA) response. Endogenous protein-coding gene and transposon transcripts exhibit Piwi-dependent endo-siRNAs at sites complementary to piRNAs and are de-repressed in Piwi mutants. Genomic loci of piRNA biogenesis are depleted of protein-coding genes and tend to overlap the start and end of transposons in sense and antisense, respectively. Our data suggest that nematode piRNA clusters are evolving to generate piRNAs against active mobile elements. Thus, piRNAs provide heritable, sequence-specific triggers for RNAi in *C. elegans*.

The Piwi/piRNA pathway has an evolutionarily conserved role in germline transposon silencing in animals. *C. elegans* encodes two Piwi family proteins, PRG-1 and PRG-2, although PRG-2 has likely little or no function (*1*, *2*). PRG-1 and piRNA expression is restricted to the male and female germline. The piRNAs of *C. elegans* are 21 nucleotides in length with a 5′ uracil (21U-RNAs) (*1–4*). In *C. elegans* piRNAs have a sequence motif, situated ~40 bp upstream of each piRNA locus, that is thought to be required for piRNA biogenesis (*2*, *3*). A challenge in the field is to understand the mechanism(s) by which piRNAs act on their targets. Proposed functions for Piwi/piRNA complexes include the RNAi-like slicing of RNA transcripts (*5–7*), transcript deadenylation (*8*) and de novo DNA methylation (*9*, *10*). Here we identify the targeting mechanism and the endogenous targets of *C. elegans* piRNAs.

We generated *C. elegans* strains carrying GFP-histone H2B fusion transgenes into which we inserted a short sequence complementary to an endogenous piRNA (21UR-1) or its reverse complement, hereafter referred to as the piRNA sensor and control sensor, respectively (see fig. S1, supplementary online text) (*11*). While the control sensor expressed nuclear, chromatin-associated GFP throughout germline development, GFP expression was silenced in animals carrying the piRNA sensor transgene (Fig. 1A,B). piRNA sensor silencing was dependent on *prg-1*. In contrast, *prg-2* did not show an effect (fig. S2, supplementary online text). An independent sensor for the unrelated endogenous piRNA 21UR-1349 confirmed these results (Fig. 1C,D).

We analyzed small RNA populations in the sensor strains by high-throughput sequencing (Fig. 1E) (*11*). We detected a set of small RNAs that map unambiguously to the piRNA sensor mRNA, mostly within ~20 bp of the piRNA target site. These small RNAs were predominantly 22 nucleotides in length with a 5′ guanosine, characteristic features of sec-ondary endo-siRNAs, also referred to as 22G-RNAs (Fig. 1F). 22G-RNAs represent the most abundant class of endogenous small RNAs in *C. elegans*, are RNA-dependent RNA polymerase products and have a 5′ triphosphate (*12–14*). The set of 22G-RNAs that map in close proximity to the piRNA target site was dependent on *prg-1* and absent in the control sensor (Fig. 1E). We validated the high-throughput sequencing data using Northern blotting for an abundant 22G-RNA mapping to the piRNA sensor (Fig. 1G). As endo-siRNA silencing can involve post-transcriptional regulation of mRNAs (*15*) or co-transcriptional gene regulation (*16*) we tested if the piRNA sensor was regulated at either level. We find that both primary transcript and mRNA are upregulated in *prg-1* mutants, consistent with co-transcriptional or a combination of post- and co-transcriptional regulation of the piRNA (Fig. 1H).

To investigate the role of endo-siRNAs in piRNA-mediated gene silencing we screened a set of 24 siRNA pathway genes. Mutants were crossed into the piRNA sensor and assayed for transgene GFP expression through fluorescent microscopy (Fig. 2A, fig. S3A,B), flow cytometry (fig. S3C,D), Northern blotting (fig. S4), or high-throughput sequencing (fig. S5). We found that a specific subset of siRNA pathway genes is required for piRNA-mediated silencing and encodes pathway components including three putative helicases (MUT-7, DRH-3, MUT-14), two RNA-dependent RNA polymerases (EGO-1 and RRF-1), the enzymes that generate secondary siRNAs, and several "worm"-specific Argonaute proteins (WAGOs) (*17*) (fig. S6A,B). While several strains with mutations in multiple WAGOs are defective in piRNA sensor silencing, *hrde-1/wago-9* is the only single mutant WAGO strain defective in piRNA sensor silencing (Fig. 2A, fig. S3). PRG-1 is necessary for both piRNA expression and sensor-specific 22G-RNA expression. In contrast, the identified siRNA pathway genes act downstream of piRNA expression and are required only for the expression of piRNA sensor-derived 22G-RNAs (fig. S4,S5). We conclude that a specific endo-siRNA pathway acts as a downstream effector of the piRNA pathway.

The Ping-Pong piRNA amplification loop in insects (*18*) and vertebrates requires endonuclease or slicing activity for biogenesis of at least a subset of piRNAs (*7*, *19*). PRG-1 contains an evolutionarily conserved DDH motif (catalytic triad) that confers endonuclease or slicing activity to some Argonaute superfamily proteins (*20*) and recombinant PRG-1 appears to have some slicing activity in vitro (fig. S7, S8, supplementary online text). To test the requirement for PRG-1 catalytic activity in vivo, we generated two transgenes expressing wild-type GFP-PRG-1 or GFP-PRG-1 DAH mutant fusion proteins (fig. S9). In *prg-1* mutants both wild-type and DAH mutant GFP-PRG-1 were sufficient to rescue piRNA expression (fig. S4). To address whether the catalytic triad of PRG-1 is required for piRNA-mediated silencing of targets we generated a second 21UR-1 piRNA sensor strain (cherrysensor) expressing mCherry-H2B. While the cherrysensor was de-silenced in a *prg-1* mu-

tant background, both wild-type GFP-PRG-1 and GFP-PRG-1 DAH restored silencing of the cherrysensor to the same extent (Fig. 2B). This was also true in the *prg-1;prg-2* double mutants (fig. S10). In addition, both wild-type and DAH mutant GFP-PRG-1 rescue the fertility defects of *prg-1* mutants (fig. S11). Finally, we generated a panel of mutated piRNA sensors and find that two mismatches are tolerated throughout the target sequence for PRG-1-dependent sensor silencing, including mismatches at positions 10 and 11 that are required for slicing (fig. S12). We conclude that PRG-1 slicing is not required in vivo.

To investigate whether piRNAs target endogenous transcripts, we considered piRNA matches in the *C. elegans* genome allowing for up to 3 mismatches. For 16,003 piRNAs we identified a total of 681,746 sites (Additional Data Table S1, S2). We found that PRG-1-dependent 22G-RNAs localize in close proximity to imperfect piRNA matches, recapitulating our observations for the piRNA sensor (Fig. 3A, fig. S13). To assess how many of these represent functional target sites, we compared genomic matches of piRNAs to those of matched control sequences. In wild-type animals, approximately 4.2%, 2.6%, 2.0% and 1.7% of the 0, 1, 2 and 3 mismatch sites exhibit unambiguously mapping 22G-RNAs, corresponding to an enrichment of 1.6, 1.4, 1.5 and 1.2 compared to control sites, respectively (Fig. 3B). In *prg-1* mutants the percentage of genomic piRNA matches with 22G-RNAs was comparable to control sites. The distribution of piRNA matches (and those with 22G-RNAs) across the genome resembled that of controls, except for an enrichment of perfect piRNA matches in the two piRNA clusters on chromosome IV (fig. S14, S15).

To further investigate mismatch tolerance of piRNA targeting we considered genomic piRNA matches with up to five mismatches. We observed that levels of PRG-1-dependent 22G-RNAs decrease with increasing number of mismatches (Fig. 3C). Levels of PRG-1-dependent 22G-RNAs were greater at sites with four compared to five mismatches, suggesting that in some cases sites with up to four mismatches can be sufficient for the synthesis of 22G-RNAs. We also observed that levels of 22G-RNAs depend on piRNA abundance (Fig. 3D).

We identified candidate endogenous targets by searching for antisense piRNA matches in annotated protein-coding genes, pseudogenes and transposons allowing for up to three mismatches (Additional Data Table S3, S4, S5). We found that in *prg-1* mutant animals 22G-RNAs antisense to candidate targets showed a stronger reduction at target sites (within 20 nt) compared to regions distant from target sites (fig. S16). When analyzing mRNA expression differences between *prg-1; prg-2* mutant and wild-type animals by microarray, mRNA expression changes showed stronger correlation with changes in 22G-RNAs at target sites compared to the whole transcript (fig. S16).

We ranked transposons and protein-coding genes by the decrease in target-site associated 22G-RNA density in *prg-1* mutant compared to wild-type animals and examined individual candidate targets (Fig. 4A,B). Transposase mRNA from Tc3 is de-silenced in *prg-1* mutants and Tc3 exhibits PRG-1-dependent 22G-RNAs against its terminal inverted repeats (TIRs) but no matching piRNAs (*1, 2*). We identified three piRNAs with imperfect complementarity to the consensus sequence of Tc3, all of which map to the TIRs, suggesting that these piRNAs target Tc3 elements *in trans*. We chose five transposable elements (CEREP1A, MARINCE1, TURMOIL1, Chapaev-2_CE, LINE2H_CE) and six protein-coding genes (*bath-45, zfp-1,* C18H2.2, *nfm-1,* Y75B8A.19, *pan-1*) with strong reduction in target-site associated 22G-RNAs for analysis by quantitative RT-PCR (Fig. 4C,D,E). Six of these candidates showed statistically significant increased expression in *prg-1* mutants ($P < 0.05$, two-sided *t*-test). We tested the requirement of an intact catalytic triad and found that both wild-type and DAH mutant GFP-PRG-1 restored silencing of *zfp-1* (F54F2.2b) in *prg-1* mutants, while an independent isoform lacking target-site associated 22G-RNAs (F54F2.2a) showed no change in expression (Fig. 4E). In addition, we

found that expression of a PRG-1-dependent 22G-RNA against *zfp-1* (F54F2.2b) was restored by both wild-type and DAH mutant GFP-PRG-1 (fig. S4). Thus, piRNAs target endogenous transcripts *in trans* for silencing, independently of slicing activity.

Our findings raise the question of how piRNAs and target sites arise during evolution. The majority of the 16,003 *C. elegans* piRNAs (96%) map to unique locations in the genome and are depleted of protein-coding genes (*2*). We confirmed that piRNA loci are depleted of protein-coding genes in both *C. elegans* and the related nematode species *C. briggsae* when compared to loci of matched control sequences (Fig. 4F). However, we did not observe a depletion of pseudogenes or transposons. piRNA loci showed a trend for depletion at the start and end of full-length DNA transposons in antisense and sense, respectively, and an inverse trend for enrichment at the start and end in sense and antisense, respectively (Fig. 4F). This signature suggests recent DNA transposon integrations downstream of instances of the sequence motif thought to be required for piRNA biogenesis. Such integrations may result in the birth of a piRNA either sense to the 5′ end or antisense to the 3′ end of the transposon. In the latter case the new piRNA has the potential to target and silence the mobile element. Indeed, the observed distances between piRNA locus and start or end of the transposon are consistent with transposon insertions downstream of existing sequence motifs (Fig. 4G, fig. S17). A similar signature was observed in *C. briggsae* (Fig. 4G, fig. S18) despite that neither piRNAs nor transposable elements are conserved between the two species. When considering imperfect piRNA matches we observed a depletion antisense to protein-coding genes (Fig. 4F, fig. S19), suggesting mRNA targeting is often detrimental and piRNAs and sites with potential for mRNA silencing undergo negative selection.

Our data demonstrate that *C. elegans* piRNAs silence endogenous transcripts by triggering a secondary siRNA response (fig. S20). While we find that individual mRNAs are piRNA targets, the physiological roles of piRNA-mediated gene regulation remain to be explored. RNAi pathways are able to silence repetitive elements regardless of their sequence content but rely on the formation of double-stranded RNA. The piRNA pathway may provide an alternative defense mechanism that is heritable and sequence-specific based on the evolution of new piRNAs against active mobile elements. Secondary siRNA amplification ensures effective silencing of abundant targets, resembling the Ping-pong piRNA amplification cycle in other species.

References and Notes
1. P. P. Das *et al.*, Piwi and piRNAs act upstream of an endogenous siRNA pathway to suppress Tc3 transposon mobility in the Caenorhabditis elegans germline. *Mol. Cell* **31**, 79 (2008). doi:10.1016/j.molcel.2008.06.003 Medline
2. P. J. Batista *et al.*, PRG-1 and 21U-RNAs interact to form the piRNA complex required for fertility in C. elegans. *Mol. Cell* **31**, 67 (2008). doi:10.1016/j.molcel.2008.06.002 Medline
3. J. G. Ruby *et al.*, Large-scale sequencing reveals 21U-RNAs and additional microRNAs and endogenous siRNAs in C. elegans. *Cell* **127**, 1193 (2006). doi:10.1016/j.cell.2006.10.040 Medline
4. G. Wang, V. Reinke, A C. elegans Piwi, PRG-1, regulates 21U-RNAs during spermatogenesis. *Curr. Biol.* **18**, 861 (2008). doi:10.1016/j.cub.2008.05.009 Medline
5. J. Brennecke *et al.*, Discrete small RNA-generating loci as master regulators of transposon activity in Drosophila. *Cell* **128**, 1089 (2007). doi:10.1016/j.cell.2007.01.043 Medline
6. L. S. Gunawardane *et al.*, A slicer-mediated mechanism for repeat-associated siRNA 5′ end formation in Drosophila. *Science* **315**, 1587 (2007). doi:10.1126/science.1140494 Medline
7. M. Reuter *et al.*, Miwi catalysis is required for piRNA amplification-independent LINE1 transposon silencing. *Nature* **480**, 264 (2011). doi:10.1038/nature10672 Medline
8. C. Rouget *et al.*, Maternal mRNA deadenylation and decay by the piRNA pathway in the early Drosophila embryo. *Nature* **467**, 1128 (2010). doi:10.1038/nature09465 Medline

9. A. A. Aravin *et al*., A piRNA pathway primed by individual transposons is linked to de novo DNA methylation in mice. *Mol. Cell* **31**, 785 (2008). doi:10.1016/j.molcel.2008.09.003 Medline

10. S. Kuramochi-Miyagawa *et al*., DNA methylation of retrotransposon genes is regulated by Piwi family members MILI and MIWI2 in murine fetal testes. *Genes Dev.* **22**, 908 (2008). doi:10.1101/gad.1640708 Medline

11. Materials and methods are available as supplementary material on *Science* Online.

12. W. Gu *et al*., Distinct argonaute-mediated 22G-RNA pathways direct genome surveillance in the C. elegans germline. *Mol. Cell* **36**, 231 (2009). doi:10.1016/j.molcel.2009.09.020 Medline

13. J. Pak, A. Fire, Distinct populations of primary and secondary effectors during RNAi in C. elegans. *Science* **315**, 241 (2007). doi:10.1126/science.1132839 Medline

14. T. Sijen, F. A. Steiner, K. L. Thijssen, R. H. A. Plasterk, Secondary siRNAs result from unprimed RNA synthesis and form a distinct class. *Science* **315**, 244 (2007). doi:10.1126/science.1136699 Medline

15. A. Fire *et al*., Potent and specific genetic interference by double-stranded RNA in Caenorhabditis elegans. *Nature* **391**, 806 (1998). doi:10.1038/35888 Medline

16. S. Guang *et al*., Small regulatory RNAs inhibit RNA polymerase II during the elongation phase of transcription. *Nature* **465**, 1097 (2010). doi:10.1038/nature09095 Medline

17. E. Yigit *et al*., Analysis of the C. elegans Argonaute family reveals that distinct Argonautes act sequentially during RNAi. *Cell* **127**, 747 (2006). doi:10.1016/j.cell.2006.09.033 Medline

18. K. Saito *et al*., A regulatory circuit for piwi by the large Maf gene traffic jam in Drosophila. *Nature* **461**, 1296 (2009). doi:10.1038/nature08501 Medline

19. S. De Fazio *et al*., The endonuclease activity of Mili fuels piRNA amplification that silences LINE1 elements. *Nature* **480**, 259 (2011). doi:10.1038/nature10547 Medline

20. J. J. Song, S. K. Smith, G. J. Hannon, L. Joshua-Tor, Crystal structure of Argonaute and its implications for RISC slicer activity. *Science* **305**, 1434 (2004). doi:10.1126/science.1102514 Medline

21. W. Wood, *The Nematode Caenorhabditis elegans* (Cold Spring Harbor Laboratory Press, 1988).

22. C. Frøkjær-Jensen *et al*., Single-copy insertion of transgenes in Caenorhabditis elegans. *Nat. Genet.* **40**, 1375 (2008). doi:10.1038/ng.248 Medline

23. C. Frøkjær-Jensen, M. W. Davis, M. Ailion, E. M. Jorgensen, Improved Mos1-mediated transgenesis in C. elegans. *Nat. Methods* **9**, 117 (2012). doi:10.1038/nmeth.1865 Medline

24. H. R. Horvitz, J. E. Sulston, Isolation and genetic characterization of cell-lineage mutants of the nematode Caenorhabditis elegans. *Genetics* **96**, 435 (1980). Medline

25. G. S. Pall, A. J. Hamilton, Improved northern blot method for enhanced detection of small RNA. *Nat. Protoc.* **3**, 1077 (2008). doi:10.1038/nprot.2008.67 Medline

26. B. Haley, G. Tang, P. D. Zamore, In vitro analysis of RNA interference in Drosophila melanogaster. *Methods* **30**, 330 (2003). doi:10.1016/S1046-2023(03)00052-5 Medline

27. K. Miyoshi, H. Tsukumo, T. Nagami, H. Siomi, M. C. Siomi, Slicer function of Drosophila Argonautes and its involvement in RISC formation. *Genes Dev.* **19**, 2837 (2005). doi:10.1101/gad.1370605 Medline

28. B. Langmead, C. Trapnell, M. Pop, S. L. Salzberg, Ultrafast and memory-efficient alignment of short DNA sequences to the human genome. *Genome Biol.* **10**, R25 (2009). doi:10.1186/gb-2009-10-3-r25 Medline

29. S. Anders, W. Huber, Differential expression analysis for sequence count data. *Genome Biol.* **11**, R106 (2010). doi:10.1186/gb-2010-11-10-r106 Medline

30. R. Gentleman, Bioinformatics and Computational Biology Solutions using R and Bioconductor (Springer Verlag, 2005).
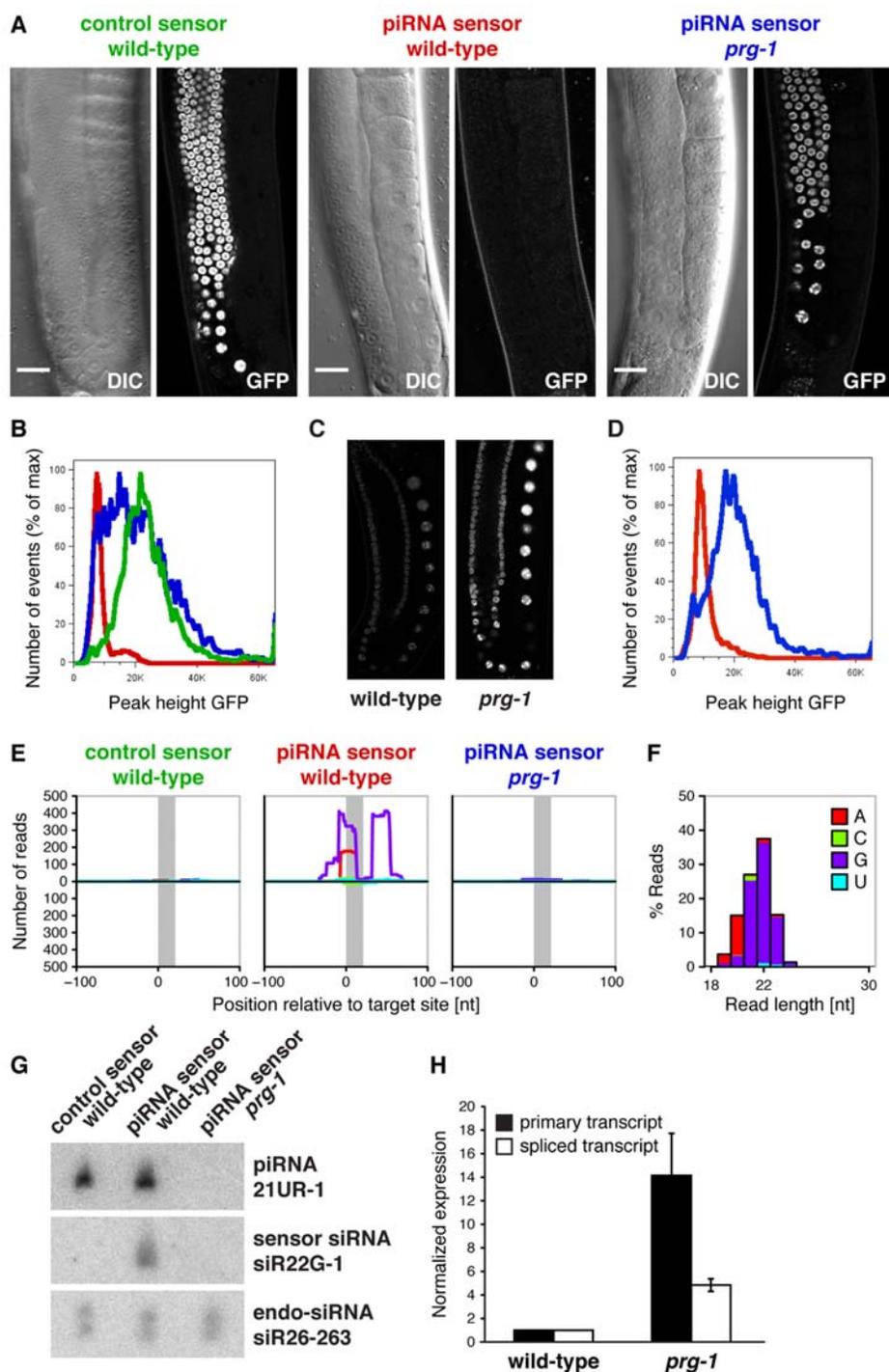
Supplementary Materials

Fig. 1. A single antisense piRNA site is sufficient for target silencing in vivo. (**A**) Fluorescence microscopy (GFP-H2B) and differential interference contrast (DIC) images of adult hermaphrodites. Scale bar 20 μm. (**B**) Flow cytometry analysis of control sensor strain (green) and piRNA sensor strain in wild-type (red) or *prg-1* (*n4357*) mutant background (blue) as in (A). (**C**) Germline GFP-H2B expression of the 21UR-1349 piRNA sensor. (**D**) Flow cytometry analysis of the 21UR-1349 piRNA sensor strain in wild-type (red) and *prg-1* mutant (blue). (**E**) Profiles of small RNA high-throughput sequencing reads with unique match to the sensor relative to the target site (indicated in grey). Colors correspond to 5′ nucleotides as indicated in the color key in (F). Positive and negative *y*-axes correspond to antisense and sense reads, respectively. (**F**) Length and 5′ nucleotide identity of small RNAs antisense to the piRNA sensor in wild-type. (**G**) Northern blot of total RNA. Probes were against piRNA 21UR-1, a piRNA sensor-specific 22G-RNA and the PRG-1-independent endo-siRNA siR26-263. (**H**) qRT-PCR of primary piRNA sensor transcript and mRNA. Data were normalized to wild-type transcript levels. Error bars are standard errors of the mean.
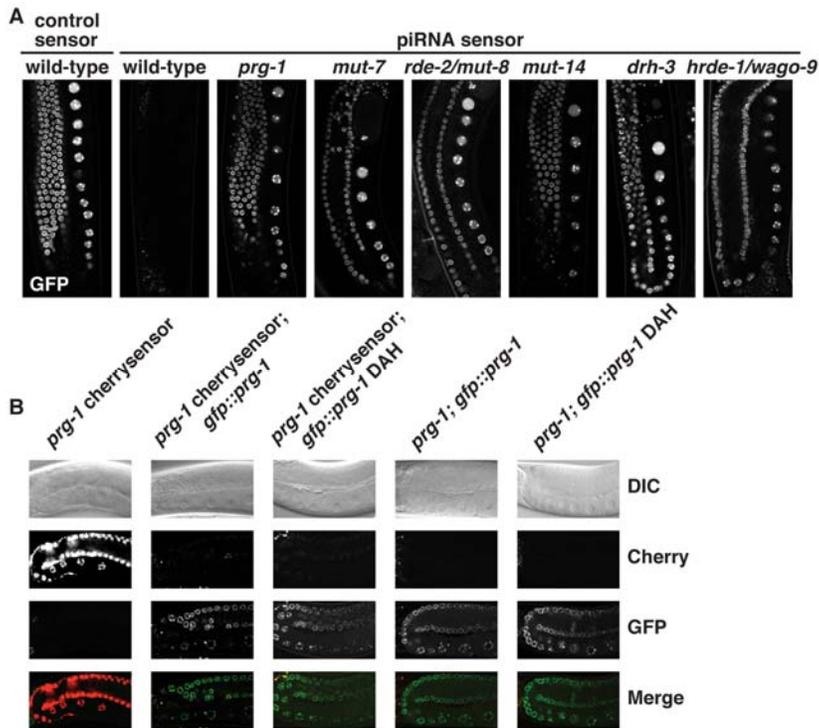
Fig. 2. A specific endo-siRNA pathway acts downstream of and is required for piRNA-mediated silencing. (**A**) piRNA sensor expression in siRNA pathway mutants as in Fig. 1A. (**B**) A second 21UR-1 piRNA sensor strain (cherrysensor) expressing mCherry-H2B in *prg-1 (n4357)*.

Fig. 3. piRNAs initiate a localized secondary siRNA response against endogenous transcripts. (**A**) Average profiles of collapsed small RNAs mapping uniquely to imperfect genomic piRNA matches (1-3 mismatches) in wild-type (left) and *prg-1* mutant (right). Top and bottom panels to the right of each profile illustrate characteristics of antisense and sense small RNAs, respectively. (**B**) Number of genomic piRNA matches (left) and percentage of matches with uniquely mapping 22G-RNAs in wild-type (middle) and *prg-1* (right). Black and white bars correspond to piRNAs and matched controls, respectively. Bars for control sequences indicate medians, error bars the range of values obtained for 20 cohorts of control sequences. Numbers above bars indicate the fold-difference between piRNAs and controls. (**C**) Difference in 22G-RNAs mapping uniquely within 20 bp of genomic piRNA matches between *prg-1* and wild-type. Shown are boxplots of the difference in 22G-RNA reads after square root transformation (box indicates interquartile range, plot extends from 5th to 95th percentile). Asterisks indicate statistical significance ($P < 0.001$, two-sided Wilcoxon rank-sum test). (**D**) As in (C) with genomic piRNA matches grouped according to motif score of complementary piRNA (as proxy for abundance).
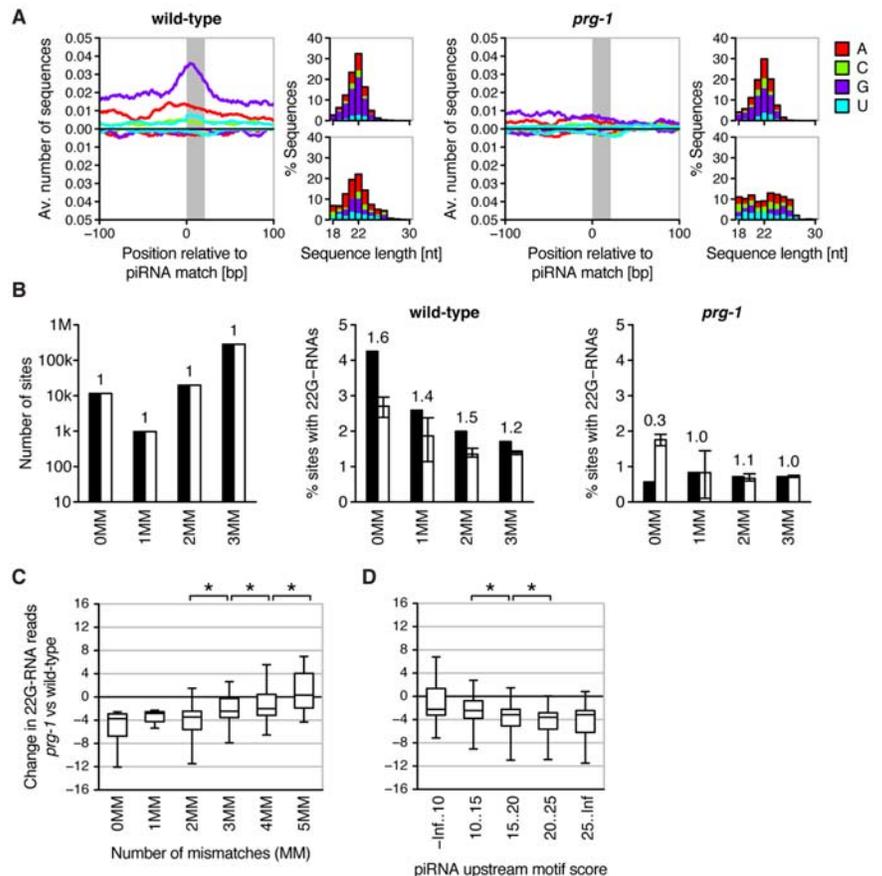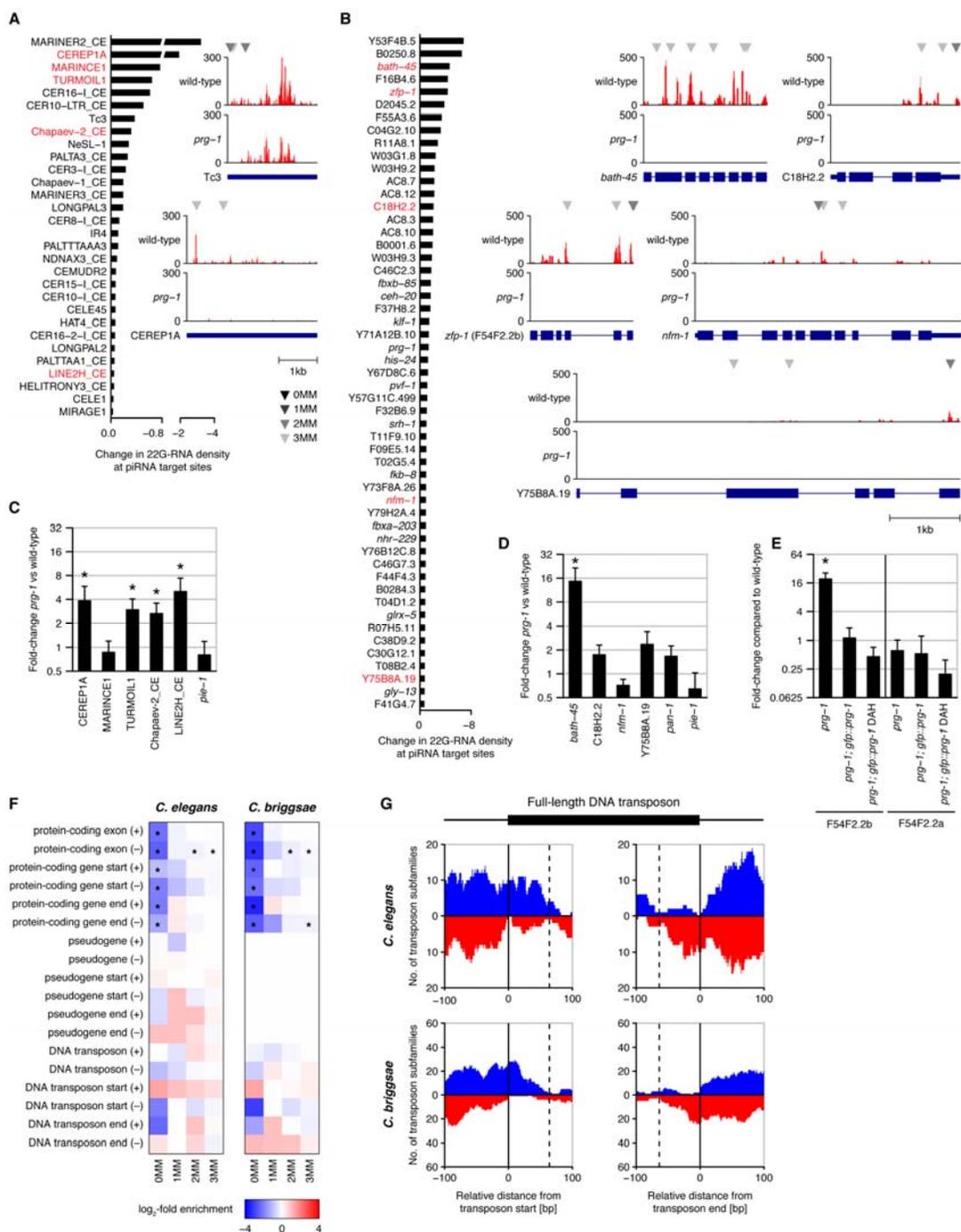
Fig. 4. Endogenous piRNA targets and piRNA evolution. (**A**) Candidate transposon targets ranked by change in 22G-RNA density at target sites between *prg-1* and wild-type. Transposons selected for qRT-PCR validation are in red. Antisense 22G-RNA profiles are shown for selected elements with target sites indicated above each profile as explained in the color key. (**B**) Candidate protein-coding targets as in (A). (**C**) qRT-PCR analysis of candidate transposon targets with fold-changes normalized to actin. Error bars are standard errors of the mean, asterisks denote *P* < 0.05 (two-sided *t*-test). (**D**) qRT-PCR analysis of candidate protein-coding targets. (**E**) qRT-PCR analysis of targeted (F54F2.2b) and non-targeted (F54F2.2a) transcripts from the *zfp-1* locus. Data were normalized to wild-type. (**F**) Enrichment and depletion of genomic piRNA matches overlapping features of interest. Red and blue indicate increased or reduced number of matches for piRNAs compared to control sequences, respectively. Asterisks indicate statistical significance. Start and end refer to the first and last 50 bp of the annotated feature, respectively. Pseudogene annotation was only available for *C. elegans.* (**G**) piRNA matches against start (left) and end (right) of DNA transposons. Profiles indicate the number of transposon subfamilies with perfect piRNA match in at least one full-length genomic copy. Positive (blue) and negative (red) *y*-axes correspond to sense and antisense matches, respectively. Dashed lines correspond to maximal allowed distance between an upstream sequence motif and piRNA 3′ end.